TOWARDS A SAFETY CASE FOR THE USE OF LASER CUTTING IN NUCLEAR DECOMMISSIONING
(A0193)

P.A.HILTON
TWI Ltd
Granta Park, Great Abington
Cambridge CB21 6AL
United Kingdom

ABSTRACT

Some of the requirements in nuclear decommissioning include size reduction of contaminated containers, pipework and other structures manufactured from stainless and other steels. Size reduction is generally performed using mechanical saws or shears, with drawbacks of quick wear, significant applied force, difficult remote operation and addition to contaminated waste mass. The use of lasers for cutting within the context of nuclear decommissioning has been recently demonstrated by TWI and others. In this paper, aspects of drawing together a safety case for using laser beams for cutting in a nuclear decommissioning cell are discussed, via analysis of relevant purpose designed experimental data. Data presented includes assessment of the use of different focal length lenses and the power densities anticipated at distances of up to 3m from the focal point, as well as beam effects on material behind the cutting zone. An assessment of anticipated material damage from stray beams or unintended exposure to laser light of surrounding items is also presented. Finally materials for effective screening against stray beams during the cutting process have been tested for effectiveness.

1. Introduction

Since 2009, TWI Ltd. and others have demonstrated the potential of laser cutting for size reduction in nuclear decommissioning. [1, 2, 3, 4, 5]. However, it is not clear if this technique has in fact yet been used for size reduction in an active environment. Although the papers cited above demonstrate the benefits of laser cutting, such as ease of automation, high process speeds, minimum fume and lack of reaction force from the cutting tool on the material being cut, from the safety case point of view, there are some drawbacks to using laser beams for cutting. These include, but are not limited to, the effects of ‘stray’ beams that pass through the material being cut and impinge on something behind the cutting point, the temperature rise in the material being cut and the effects of the sparks generated in the laser cutting process. In addition, the amount of dross (material removed from the cut kerf) accumulated and fume generated and how this is dealt with are also of concern, but will not be discussed further in this paper.

The paper includes the results of a series of experiments performed to generate safety case useful information for the use of a 5kW fibre laser and its beam delivery system, in the application of laser cutting of CMn and stainless steels. In any laser cutting process, it is possible that the laser beam will be released while not incident on the material being cut, for example when performing single sided tube cutting, or when initiating a cut from the edge of plate material. During the time the beam is released without cutting, the laser beam will propagate past the focal point, diverging with increasing distance (and hence reduced power density). In this condition the laser beam will eventually impinge, either on the wall or floor of the cell in which the cutting is taking place or it will hit something else behind the cutting point. Once the cutting starts, energy will be removed from the beam, but to make a cut, the beam must pass through the material and hence some energy, albeit reduced, will propagate past the material for the duration of the cut.

Work has therefore been conducted to measure the effects of such 'stray' beams on materials which might be found in a typical nuclear cell or cave. Firstly, methods are described to determine the power density available in the laser beam at a given distance from the cutting point. This involves measurement of the laser beam diameter at various points along its path. The effects of such beams on materials which might be used to register 'beam diameter', by positioning them at various distances behind the focus position, are then described and indications given of the correlation of 'beam diameter' to such imprints. The paper goes on to describe measurements of temperature rise due to stationary and moving laser beams using infrared spot pyrometry, before assessing the effects of the beams on materials which might be placed after the cutting point, acting as beam 'arresters', to safely absorb the laser energy arising from 'stray' beams. Finally, by way of example, the concept of a 'safety' sphere for laser cutting is introduced.

2. Experimental arrangements

The laser cutting system used for these experiments consisted of a 5kW industrial fibre laser, (emitting laser light at 1micron wavelength), a delivery fibre of diameter 150 microns, a collimating lens of 120mm focal length a focusing lens of 250mm focal length. The lens system was contained in a cutting head, typical of that described in refs [2-5]. With such an optical beam delivery system, the diameter of the smallest focused spot is calculated from the ratios of the focal lengths of the collimating and focusing lenses and the delivery fibre diameter, and in this case is ~0.3mm diameter. The corresponding power density in this spot is ~70kW/mm^2, at a power of 5kW. With the type of laser used, the spot at focus, will have a 'top hat' shaped energy distribution, but away from the focus, the energy distribution across the beam becomes more Gaussian in form. Because of the Gaussian form, the definition of the diameter of the beam requires some clarification. In Gaussian optics the beam diameter is stated to be the diameter at which the intensity of the beam reaches a value $1/e^2$ of the peak intensity. By definition, in a real beam, this means there is always some intensity outside this calculated 'diameter'.

In the experiments reported below, the optical systems described above have been used on a variety of materials, at distances from the beam focus from 200 to 3000mm. In some experiments the beams were stationary and in some the beams were moving. The materials used in the tests are listed below, although not all these were used in every experiment:

- CMn and 304 stainless steel plate.
- Graphite plate and thin, flexible exfoliated graphite sheet.
- Cast concrete.
- Three types of fire resistant fibrous material - typical of the type used in fire doors.
- Thin aluminium and steel plate with different applied coatings, including paint and anodizing.

3. Experiments Performed

3.1 Determination of the beam diameter

The objective of this series of experiments was to compare the measured beam diameters at various distances after the beam focus, to real imprints of the laser beam on various materials which might be candidates as targets to establish the beam diameter using a simple 'imprint' technique. To measure the beam diameter at a given distance, a mirror edge was passed transversely through the propagating beam while the power transmitted past this edge was constantly measured. The mirror slowly reveals or hides the beam. The recorded power measurement is essentially the volume integral of the beam intensity. Hence by mathematical regression of the integral equation against the measured power per mirror displacement, the intensity profile of the laser beam can be established at ant point. Fig. 1 is a typical plot of the power recorded by the detector, in this case for an incident 1kW laser beam, at a distance 260mm below the beam focus, with the intensity profile and the fitted Gaussian curve derived from the power measurements.

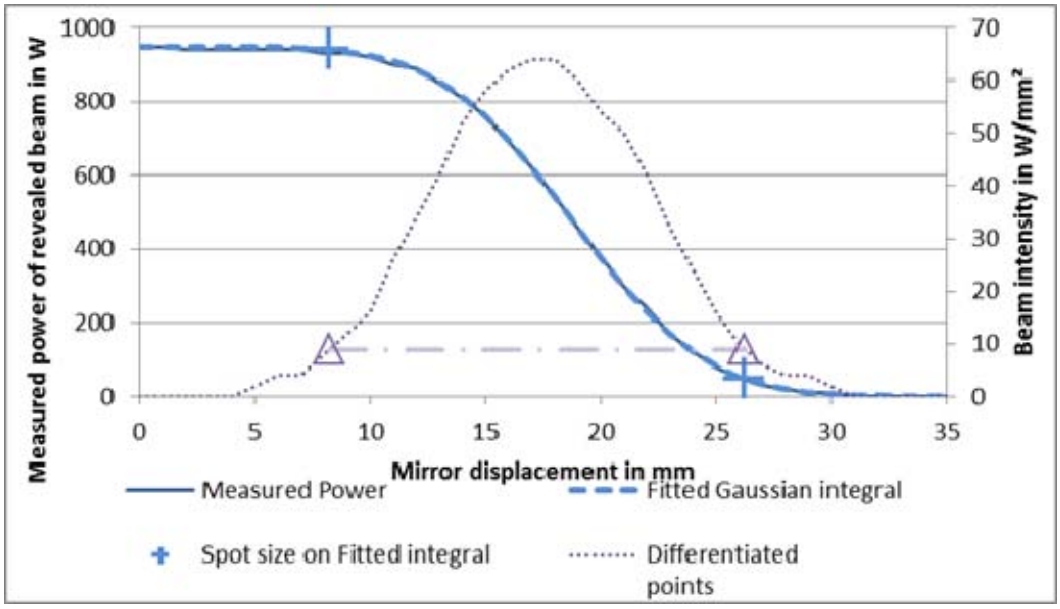

Fig.1. Beam power measurement as a function of mirror position (solid line) and corresponding fitted Gaussian integral (dashed line). The dotted line is the differentiated points representing the beam profile. The $1/e^2$ beam diameter is marked between the triangles.

Two of the materials used for trials to determine their suitability for beam imprints were calcium silicate based board (Vermiculux), and steel sheet, spray painted black.

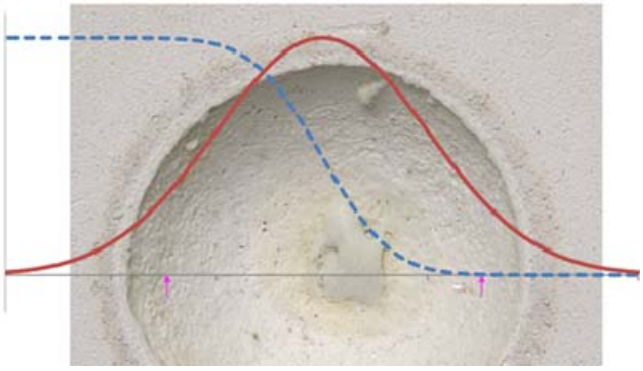

Fig. 2. Laser beam induced imprint on calcium silicate based material with corresponding beam intensity profile. The calculated beam diameter (shown between the two small arrows) was 18.25mm.

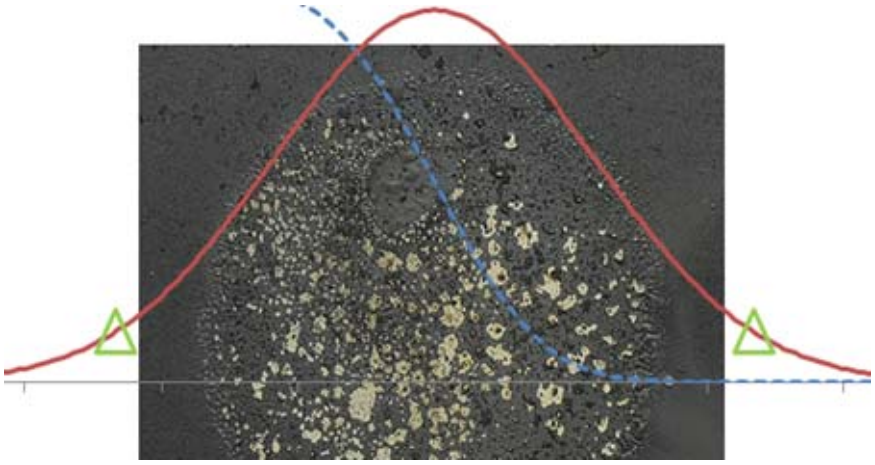

Fig. 3. Laser beam induced imprint on painted steel sheet with corresponding beam intensity profile. The calculated beam diameter (shown between the two triangles) was 116mm.

Fig. 2 shows the effect on the calcium silicate material of an incident 5kW beam for 1s duration. The material was positioned 260mm below the laser beam focus. Onto this image is superimposed the laser beam intensity profile derived at the same position. It is clear that the 'diameter' of the imprint of the beam on the material is larger than the beam diameter calculated from the profile, indicated by the two small arrows, which corresponds to 18.25mm. Fig.3 shows the effect of an incident 5kW laser beam, for the same duration, on black spray painted steel. In this case the measured beam diameter (between the triangles) was measured at 116mm (corresponding to a measuring distance of about 1700mm from the beam focus. In this case it is clear that the beam imprint 'diameter' as reflected on this particular substrate is smaller than the fitted beam diameter.

This work shows the difficulty of selecting a material suitable for imprint measurements of beam diameter, and which would be useful over a range of distances. If this method is chosen to establish beam diameter, and subsequently beam intensity, then it is recommended that the same material is always used and reference imprints are created at a set of given distances away from beam focus, for which measurements of beam diameter have previously been determined by alternative means. Of the materials tested the most appropriate, which showed consistency over a large range of distances, was black anodised aluminium.

3.2 Measurement of temperature rise due to incident laser beams

3.2.1 Beam stationary

For these trials an infrared spot pyrometer (IMPAC IPE140 MB10), sensitive away from the laser wavelength, was used to measure surface temperature on CMn steel, concrete and graphite. The sensor spot had a diameter of 2mm. The pyrometer focus was concentric with the beam irradiated area and the sample plane was positioned at four different angles to the incident beam. Experiments consisted of turning on the data acquisition from the pyrometer and then irradiating the sample, at a given distance from the beam focus, with a given power, for a given time. Temperature rise times and fall times (after switching off the beam) were recorded (although the latter are not presented here) and the rates of temperature rise and fall calculated. The results for temperature rise time are presented in Figs. 4, 5 and 6 below, for steel, graphite and concrete surfaces respectively.

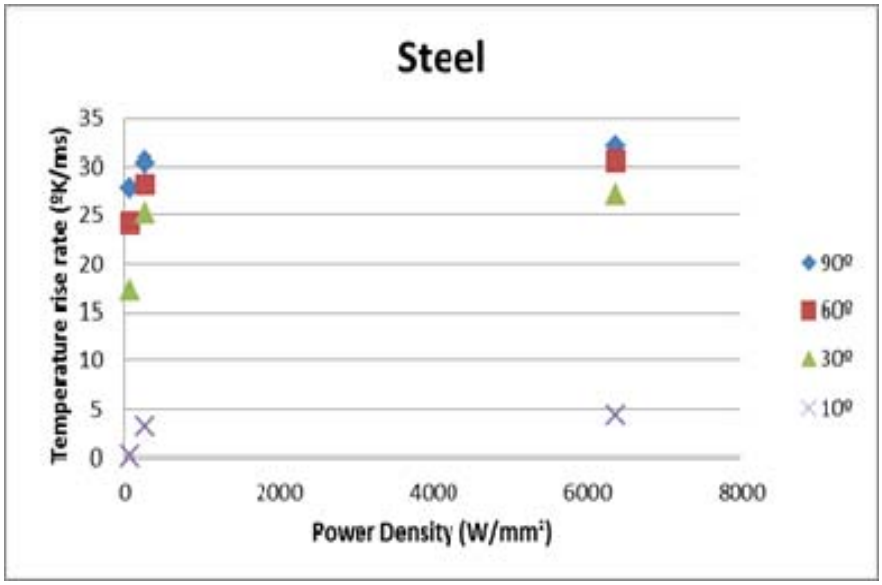

Fig. 4. Rate of temperature rise for steel (15mm thickness), for an incident 5kW beam as a function of applied power density, at various angles of incidence.

Generally, as the beam gets larger in diameter, the rate of recorded temperature rise drops and more pronounced drop is seen as the beam approaches the grazing angle. The

relationships appear to follow a non-linear trend similar to the sine of the illumination angle. It is also evident that when irradiating with a 5kW beam at angles larger than 30º from the sample surface and distances smaller than 0.5m from the focal point, exposure times of 1s can cause damage to any of the three materials.

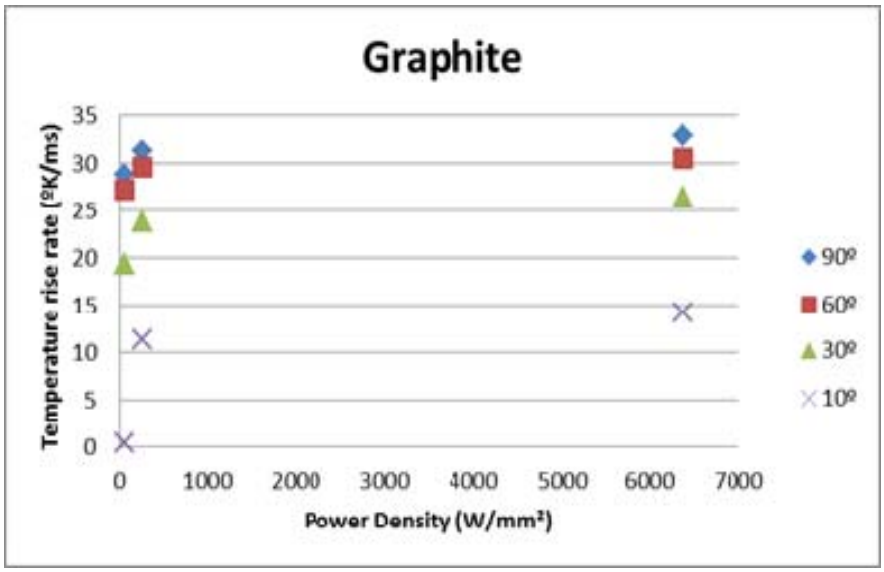

Fig. 5. Rate of temperature rise for graphite (12mm thickness), for an incident 5kW beam as a function of applied power density, at various angles of incidence.

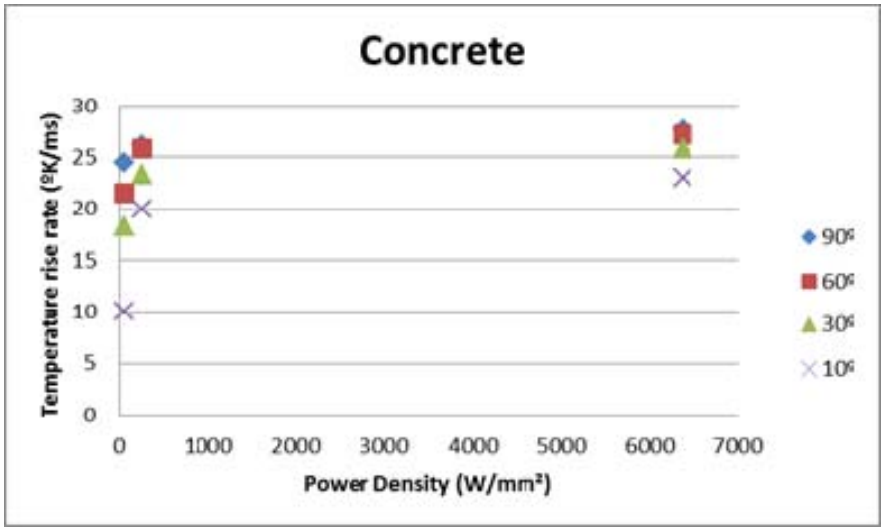

Fig. 6. Rate of temperature rise for concrete (45mm thickness), for an incident 5kW beam as a function of applied power density, at various angles of incidence.

This work has shown that the temperature rise imposed by a laser beam incident on each of these materials can be significant and enough to cause damage. For steel and graphite, these effects are reduced for larger angles of incidence when compared to concrete. This implies that effort might need to be directed at protecting concrete walls in cells were laser cutting is envisaged. The best material for protection would be graphite plate or possibly steel.

3.2.2 Moving beam

Trials were performed with a moving beam with a moderately defocussed laser beam diameter of 5mm and a stationary pyrometer spot. Data was obtained on steel plate, of 15mm thickness, with incident beam powers of 1 and 3kW. The results for the 1kW beam are plotted in Fig. 7, which shows the recorded temperature rise and fall for three different travel speeds

as a function of time. When comparing the results for the two different powers, the time the material spends above 200ºC can be noted. For example, the 1kW beam this is 2.5, 3.8 and 13s, for speeds of 1500, 500 and 100mm/min respectively. For the 3kW beam this is 4, 6.8 and 50s respectively. For the slowest speed, the time spent above 200ºC is 285% longer for the 3kW beam than for the 1kW beam. For the fastest speed, the difference is 60%. Hence there appears to be a logarithmic relationship between travel speed and maintaining temperature above a certain level.

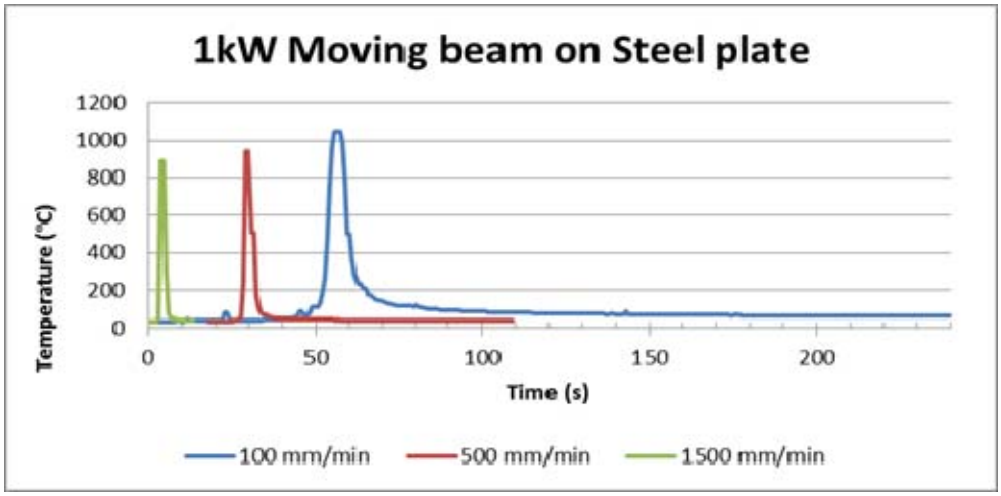

Fig.7. Temperature monitoring of a 15mm thickness steel plate while passing a 1kW beam of 5mm diameter spot size at various speeds, over the pyrometer sensor.

This work has shown that the impact of a moving beam on a material surface is much less than for a stationary beam. It also shows that more heat will be deposited into the material the slower the speed of the moving beam, which could affect material degradation.

3.3 Measurements on potential beam arrester materials

Tests were performed on different materials to assess their potential use as beam arresters. The tests were designed to characterise the capability of the materials to withstand laser illumination at levels up to 5kW kilowatts and distances from the focal point of twice the focal length or more. The following materials were tested:

- Graphite panel (thick)
- Steel plate (thick)
- Molybdenum sheet (representing refractory metals)
- Black anodised aluminium sheet (thin)
- Graphoil® - exfoliated graphite sheet (thin)
- Filtron® - perspex sheet loaded with infrared absorbing dye (for placing over cell windows)
- Concrete slab

Each material was tested to a maximum distance of 3m from the laser focal point, using a stationary beam. The highest recorded temperatures, rise times to those temperatures and illumination durations that achieved a visible mark on the material surface and visible degradation of the material surface, were recorded for each material. Indications of the power density causing this condition, for each distance from focus, were calculated from the fitted model of the beam diameter derived in Section 3.1 above, and the applied power. The tables below list the results obtained for the materials stated above for a laser power of 5kW. For some materials like graphite, Graphoil® and the molybdenum sheet, the maximum temperature recorded at higher power densities, was 1000ºC, as the pyrometer sensors used saturated at that point. The maximum exposure time was 30min. In Table 1 N/V means nothing significantly visible on the surface.

0.5m Distance from focus – 4.7W/mm² power density				
Material	**Highest Temperature (ºC)**	**Rise time to highest temperature (s)**	**Time to mark surface (s)**	**Material deterioration duration (s)**
Graphite plate	Sensor saturated	0.07	0.1	~300
Steel plate	1000	0.1	0.1	30
Mo Sheet	Sensor saturated	1	0.01	~120
Blackened Al	340	0.01	0.1	20
Graphoil	Sensor saturated	0.1	0.01	~300
Filtron	412	0.2	0.001	1
Concrete slab	Sensor saturated	1	0.01	~~1200
1m Distance from focus – 1.2W/mm² power density				
Material	**Highest Temperature (ºC)**	**Rise time to highest temperature (s)**	**Time to mark surface (s)**	**Material deterioration duration (s)**
Graphite plate	Sensor saturated	0.520	1	~1800
Steel plate	510	1	1	~180
Mo Sheet	430	1	1	~1200
Blackened Al	560	0.1	0.1	60
Graphoil	Sensor saturated	0.650	0.1	N/V
Filtron	400	0.1	0.01	4
Concrete slab	840	1	0.01	N/V
2m Distance from focus – 0.3W/mm² power density				
Material	**Highest Temperature (ºC)**	**Rise time to highest temperature (s)**	**Time to mark surface (s)**	**Material deterioration duration (s)**
Graphite plate	400	1	N/V	N/V
Steel plate	180	1	30	N/V
Mo Sheet	100	1	N/V	N/V
Blackened Al	130	0.1	1	N/V
Graphoil	320	1	1	N/V
Filtron	370	1	1	20
Concrete slab	270	1	~60	N/V
3m Distance from focus – 0.133W/mm² power density				
Material	**Highest Temperature (ºC)**	**Rise time to highest temperature (s)**	**Time to mark surface (s)**	**Material deterioration duration (s)**
Graphite plate	250	1	N/V	N/V
Steel plate	70	1	N/V	N/V
Mo Sheet	N/A	N/A	N/V	N/V
Blackened Al	100	1	20	N/V
Graphoil	200	1	N/V	N/V
Filtron	240	1	1	200
Concrete slab	60	1	~180	N/V

Tab 1: Details of deterioration results on different materials for different propagation distances

In terms of suitability for acting as beam arrestor materials such as graphite, Graphoil® and molybdenum performed best in terms of withstanding exposure to high power density illumination. Graphite is a fairly cheap material and easily available in various forms. If something needs to be covered for protection Graphoil® which is a material of moderate cost that features good flexibility, good absorbance of laser light (and hence suppression of further spread of laser light), low weight and high durability against laser illumination. Black anodised aluminium is a cost effective material that can achieve some degree of beam absorption (and suppression of further spread) while demonstrating moderate durability against illumination. Filtron, which is usually used for eye protection, can be used to contain laser light (coherent light) at low intensity levels, but should not be subjected to direct illumination.

4. Extension to the Safety Sphere Concept

One possible use of the results presented above is to help in the definition of a safety sphere around a laser cutting point. Two examples are presented below, firstly, for a steel sheet acting as a beam arrestor and then for a graphite plate acting as a beam arrestor.

4.1 Case for steel

The exemplar beam delivery system consists of a 150µm diameter optical fibre, a 120mm focal length collimating lens and a 250mm focal length focussing lens, and the laser power is set at 5kW. A piece of 3mm thick steel is placed behind the sample to be cut at 1m from the anticipated position of the beam focus. The direction of illumination is normal to its surface. The beam diameter on the steel is thus going to be ~73mm. At 5kW the power density applied will be approximately 1.19W/mm². If the beam is turned on before it begins cutting, then the steel arrestor behind the process point is going to receive the maximum power density.

The material can remain in the beam safely for several seconds based on the damage thresholds recorded above. If the direct illumination is sustained for 2 to 3 minutes, the material would be expected to deteriorate significantly. By inclining the steel surface by 60 degrees, one can expect the rate of temperature rise to reduce to approximately half of that in the normal incidence condition, as the power density of the beam is relatively low. Hence, safe illumination time before material deterioration can progress might be extended to 4min, since the anticipated temperature rise time is now halved. However, part of the beam is now being reflected away from the steel arrestor and care should be taken not to direct the beam to any more sensitive materials located further away. In all conditions the steel plate would be expected to sustain surface oxidation within the first second of the illumination duration.

If the material is to be exposed only to the breakthrough beam (ie that emerging through the cut) these times will be longer, depending on how much of the beam energy is used to make the cut. For any given material and thickness this will depend very significantly on the laser power used and the cutting speed.

4.2 Case for graphite

The exemplar beam delivery system again consists of a 150µm diameter optical fibre, a 120mm focal length collimating lens and a 250mm focal length focussing lens, and the laser power is set at 5kW. The following is considered: The cutting process will start outside the material that is being cut and the beam will take 3 seconds to enter the that material. The cutting process will take 15 seconds to be completed once the beam has engaged with the material that is being cut, and then the beam will switch off. The material being cut is placed at the beam focus. A plate of graphite is positioned 500mm behind the material being cut and the beam will illuminate the graphite at normal angle of incidence. The maximum power density at the plane of the graphite is about 5W/mm². It might be expected that the graphite would withstand this irradiation for approximately 300s, without significant deterioration. Hence the graphite can be subjected to the full capacity of the beam for the whole duration of the cutting, without risking its performance integrity as a beam arrester. Minor surface damage effects might be observed on the graphite and these are expected to come about within 0.1s of illumination.

5. Conclusions

This paper describes a series of experiments conducted using a fibre laser system capable of a wide range of potential decommissioning applications, in order to develop data to support the safety case for use of such a laser in cutting active components. Materials are suggested for possible consideration as beam arresters, particularly graphite plate and exfoliated graphite flexible sheet. Methods are also suggested for determination of beam diameter, and hence applied power density, from a laser cutting system. Indications of temperature rise times induced by stray laser beams on materials which might be found in current caves or cells are also given.

6. References

1 C Chagnot, G de Dinechin, G Canneau, and J-M Idasiak, 2009: 'Dismantling nuclear power plant with new industrial cw Nd:YAG high power lasers' Proceedings of Global, Paris, France, Sept, Paper 9539.

2 Hilton P A and Walters C L. 2010: 'The laser alternative in nuclear decommissioning - tube cutting and concrete scabbling using the latest technology'. Nuclear Engineering International, Vol 55, no 672.

3 Hilton P A, Khan A and Walters C L. 2010: 'The Potential of lasers in nuclear decommissioning'. ENC, European Nuclear Conference, Barcelona, Spain, 30 May - 2 June. European Nuclear Society.

4 Hilton P A and Khan A. 2012: 'Advances in laser cutting as a decommissioning and dismantling tool' ENC. European Nuclear Conference, Manchester, UK, June. European Nuclear Society.

5 Hilton P A. 2013: 'Parameter Tolerance Evaluation when Laser Cutting in Decommissioning Applications' Proc. ICALEO, Miami, paper 501. Laser Institute of America.

7. Acknowledgements

This work was carried out as part of the LaserSnake2 collaborative research project. LaserSnake2 is co-funded by the UK's Technology Strategy Board, the Department of Energy and Climate Change, and the Nuclear Decommissioning Authority, under grant number 110128. The LaserSnake2 project includes OC Robotics, Laser Optical Engineering, ULO Ltd and the UK's national Nuclear Laboratory, as well as TWI.